Spectral framework for geothermal borehole heat exchangers

Rafid Al-Khoury
Faculty of Civil Engineering and Geosciences, Delft University of Technology, Delft, The Netherlands

Received 29 May 2009
Revised 21 September 2009
Accepted 24 September 2009

Abstract

Purpose – This paper aims to present a framework for deriving analytical and semi-numerical models for coupled conductive-convective heat transfer processes in a borehole heat exchanger subjected to general initial and boundary conditions.

Design/methodology/approach – The discrete Fourier transform and the spectral element method have been utilized for deriving two spectral models for a single U-tube borehole heat exchanger in contact with a soil mass.

Findings – Verification and numerical examples have shown that the developed models are accurate and computationally very efficient. It is illustrated that one spectral element is capable of producing results which are more accurate than those produced by 200 finite elements.

Practical implications – The gained computational efficiency and accuracy will boost considerably the possibilities for more insight into geothermal analysis, which will improve the procedure for designing competitive energy extraction systems.

Originality/value – The models are capable of calculating exactly the temperature distribution in all involved borehole heat exchanger components and their thermal interactions.

Keywords Heat exchangers, Heat conduction, Convection, Geothermal power

Paper type Research paper

1. Introduction

Borehole heat exchanger (BHE) is a geothermal heat pipe that is inserted vertically in a borehole to form a U-shaped tube and then fixed by filling the borehole with some sort of grout material. It consists of a pipe-in, where a fluid (refrigerant) coming from a heat pump enters, a pipe-out, where the refrigerant leaves the U-tube and enters into the heat pump, and a grout. The heat pump, usually located inside a building, circulates the fluid in the BHE deep into the ground. The fluid gets in contact with the surrounding soil via the grout, where conductive-convective heat transfer processes occur. The heat pump works as a heat exchanger, which extracts a designed amount of heat from the refrigerant and pumps it back to the BHE. This system has been widely used for heating and cooling of public and residential buildings.

In practice, single or double U-tube BHEs are utilized (Figure 1). They are very slender heat pipes with dimensions of the order of: U-tube diameter, 30 mm, borehole diameter, 150 mm, and borehole length, 100 m. The slenderness of the BHEs makes their installation relatively simple. However, it exerts enormous computational challenges, especially when numerical methods are utilized. As a result several theoretical and computational assumptions and approximations were conducted in order to circumvent this problem and obtain feasible solutions.

All known solution techniques, such as analytical, semi-numerical, and numerical, with different complexities and rigor, were utilized for the simulation of heat transfer processes in BHEs and the surrounding soil mass. Analytical models, such as the cylindrical heat source model introduced by Carslaw and Jaeger (1947) and the infinite line-source model developed by Ingersoll *et al.* (1954), give transient solutions to the

International Journal of Numerical Methods for Heat & Fluid Flow
Vol. 20 No. 7, 2010
pp. 773-793

0961-5539
DOI 10.1108/09615531011065566

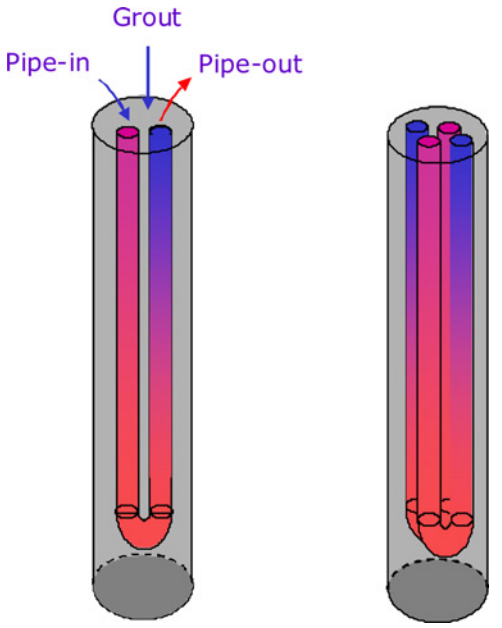

Figure 1.
Single and double BHEs

heat diffusion equation for an infinite cylinder or a line source embedded in an infinite medium. Both models are computationally intensive, although the line-source model is numerically more stable (Marcotte and Pasquier, 2008). These models have been extensively elaborated. Sutton *et al.* (2003) incorporated groundwater flow in the line-source model. Zeng *et al.* (2002, 2003) introduced analytical solution for a line source of a finite length embedded in a semi-infinite medium. Marcotte and Pasquier (2008) introduced a computationally efficient solution to finite and infinite line-source models by performing convolution in the frequency domain using the fast Fourier transform (FFT) algorithm. Recently, the finite line-source model has been extended by Marcotte and Pasquier (2009) to account for borehole inclination and borehole head located below the ground surface.

Semi-numerical solutions have been utilized by, among others, Eskilson and Claesson (1988). They utilized coupling between the Laplace transform method and the finite difference method for the simulation of thermally interacting heat extraction boreholes. Eskilson and Claesson introduced a semi-analytical function, known as the G-function, to simulate multiple BHEs embedded in an infinite medium. Their original work was limited to long time steps. Later on, it was elaborated by Yavuzturk and Spitler (1999), to account for short time steps.

Numerical solutions such as the finite difference and the finite element methods have also been utilized in this field of applications. Clauser (2002) and Sliwa and Gonet (2005), among others, developed computational models and computer codes for modeling coaxial and other types of BHEs using the finite difference method. Muraya (1994) utilized the finite element method for describing heat transfer processes in the BHE and the surrounding soil mass. Other important contributions in this field are presented in Al-Khoury *et al.* (2005).

In an earlier work (Al-Khoury *et al.* 2005; Al-Khoury and Bonnier, 2006), a computationally efficient model based on the Petrov-Galerkin's finite element method for

the analysis of heat flow in single and double geothermal U-tube BHEs was developed. The BHE was modeled using a time-space line element. However, all significant three-dimensional aspects, such as geometry and thermodynamic processes, were taken into considerations. This has allowed for the utilization of coarse meshes, alleviating thus the need for extremely fine meshes that are typically utilized in modeling such systems.

In spite of the computational efficiency of the above-mentioned work, analytical and semi-numerical solutions are yet preferable because of their little demands on computational power and ease of use in engineering practice. For this, in this publication, a framework for deriving analytical and semi-numerical models for the simulation of coupled conductive-convective heat transfer processes in a BHE subjected to general initial and boundary conditions is introduced. The spectral analysis method for solving partial differential equations is utilized. Two models are presented. The first model is derived on the basis of the discrete Fourier transform method. The second model is derived on the basis of the spectral element method (SEM). This method describes field equations in a homogeneous medium exactly. Combination of different media can be achieved using the finite element matrix formulation and assembly techniques. As such, it allows for the simulation of a BHE in contact with a multilayer system. An important feature of the developed models is their capability to calculate the temperature distribution in all involved BHE components (pipe-in, pipe-out, and grout) and their thermal interactions exactly. This feature distinguishes the introduced models from existing ones, merely those based on the cylindrical heat source and the line-source models, where only averaged temperature distribution along the BHE is calculated.

2. Boundary value problem of a borehole heat exchanger

In this section, formulation of the boundary value problem of conductive-convective heat transfer in a single U-tube BHE is presented. The governing equations describing heat transfer in the involved BHE components and their thermal interactions are first established. Then, the initial and boundary conditions, which are typically involved in shallow geothermal systems, are defined.

Governing equations. Consider a single U-tube BHE with a control volume of length dz, consisting of three pipe components (pipe-in (denoted as i), pipe-out (denoted as o), and grout (denoted as g); Figure 2). Due to the slenderness of the BHE, heat transfer is considered only along its axial axis. The radial variation of temperature is in effect negligible. The pipe components transfer heat across their cross-sectional areas and exchange fluxes across their surface areas. For a transient condition, equating the rate of thermal energy entering the control volume to the rate of energy leaving it, the net heat flow into each of the pipe components can be expressed as (Al-Khoury and Bonnier, 2006):

$$\begin{aligned}
&\rho c \frac{dT_i}{dt} dV_i - \lambda \frac{d^2 T_i}{dz^2} dV_i + \rho c u \frac{dT_i}{dz} dV_i + b_{ig}(T_i - T_g)\, dS_{ig} = 0 \\
&\rho c \frac{dT_o}{dt} dV_o - \lambda \frac{d^2 T_o}{dz^2} dV_o - \rho c u \frac{dT_o}{dz} dV_o + b_{og}(T_o - T_g)\, dS_{og} = 0 \\
&\rho c_g \frac{dT_g}{dt} dV_g - \lambda_g \frac{d^2 T_g}{dz^2} dV_g + b_{ig}(T_g - T_i)\, dS_{ig} + b_{og}(T_g - T_o)\, dS_{og} = 0
\end{aligned} \tag{1}$$

in which T_i, T_o, and T_g (K) represent the temperatures in pipe-in, pipe-out, and grout, respectively, u (m/s) denotes the refrigerant velocity, b_{ig} and b_{og} (W/m^2 K) are the reciprocal of the heat resistance between pipe-in and the grout and between pipe-out and the grout,

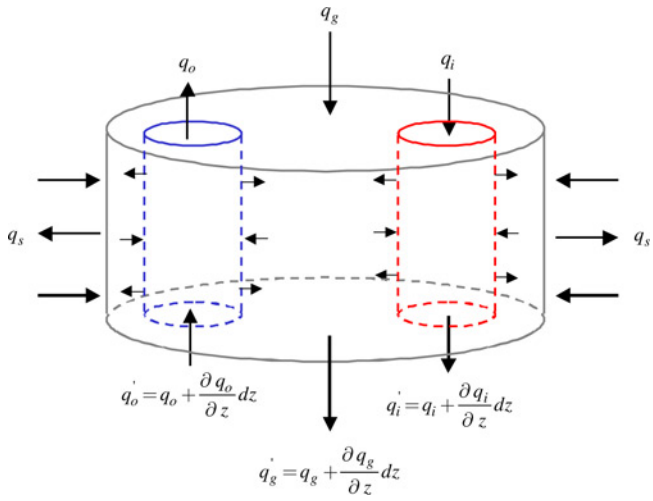

Figure 2.
Control volume of a single BHE in the z direction

respectively, c (J/kg K) is the specific heat of the fluid, ρ (kg/m^3) is the mass density of the fluid, ρc_g (J/m^3 K) is the volume heat capacity of the grout, λ and λ_g (W/m K) are the thermal conductivity of the pipe material and the grout, respectively, and dV and dS represent the volume and the surface area of the pipe components, respectively.

This formulation illustrates that there is a strong coupling between the grout and each individual pipe, and an indirect coupling between pipe-in and pipe-out via the grout. The grout works as an intermediate medium. The heat transfer coefficients for the pipe-in grout and the pipe-out grout can be described as (Al-Khoury *et al.*, 2005):

$$b_{ig} = \frac{1}{R_{ig}}, \quad b_{og} = \frac{1}{R_{og}} \tag{2}$$

where,

$$R_{ig} = R_{\text{convection}} + R_{\text{pipe material}} = \frac{1}{r_o/r_i\, h} + \frac{r_o \ln(r_o/r_i)}{\lambda_{\text{p}}} \tag{3}$$

with r_i and r_o the inner and the outer radius of the pipe, respectively, λ_{p} the thermal conductivity of the pipe material, and,

$$\bar{h} = \frac{\text{Nu}\,\lambda}{D_i} \tag{4}$$

where D_i is the inner diameter of the pipe, and Nu is the Nusselt number, which can be defined as:

$$\text{Nu} = 0.664\,\text{Re}^{1/2}\,\text{Pr}^{1/3} \quad \text{for laminar flow} \tag{5}$$

$$\text{Nu} = 0.023\,\text{Re}^{0.8}\,\text{Pr}^{0.4} \quad \text{for turbulent flow} \tag{6}$$

in which Pr is the Prandtl number and Re is the Reynolds number defined as:

$$\text{Re} \equiv \frac{u D_i}{\nu} \tag{7}$$

with u (m/s) the average refrigerant velocity, and $\nu \equiv \mu_m/\rho$ the kinematics viscosity (m^2/s) with μ_m ($N\,s/m^2$) the refrigerant mass-based viscosity and ρ (kg/m^3) its mass density. In the literature, the motion is usually considered turbulent for $Re > 2{,}000$. The same is valid for R_{og}.

Initial and boundary conditions. Initially, at time $t = 0$, the temperature distribution in the system is assumed equal to the steady-state temperature of the surrounding soil, just before the heating operation starts, i.e.,

$$T_i(z,0) = T_o(z,0) = T_g(z,0) = T_s(z,0) \tag{8}$$

in which T_s is the soil temperature immediately around the pipe.

Operational BHE system usually involves three boundary conditions. The first boundary condition describes the temperature (or heat flux) of the refrigerant coming from the heat pump, and just entering the inlet of pipe-in, such that:

$$T_i(0,t) = T_{in}(t) \tag{9}$$

The second boundary condition describes the heat transfer processes between the grout and the neighboring soil mass, as:

$$\lambda_g \frac{\partial T_g(z,t)}{\partial z} = b_{gs}[T_g(z,t) - T_s(z,t)] \tag{10}$$

in which b_{gs} is the reciprocal of the heat resistance between the soil and the grout that can be described as (Al-Khoury *et al.*, 2005):

$$b_{gs} = \frac{1}{R_{ig} + R_{og} + R_{gs}} \tag{11}$$

where R_{ig} is as described in Equation (3) (same is valid for R_{og}), and R_{gs} may take this form:

$$R_{gs} = \frac{r_g \ln(r_g/r_{eq})}{\lambda_g} \tag{12}$$

in which r_g is the radius of the grout (borehole), and $r_{eq} = \sqrt{r_{in}^2 + r_{out}^2}$ (r_{in} = pipe-in radius and r_{out} = pipe-out radius).

The third boundary condition arises from the physics of the problem. At the bottom of pipe-in, at $z = L$ (where L denotes the length of the BHE), the temperature of pipe-in is equal to the temperature of pipe-out, such that:

$$T_i(L,t) = T_o(L,t) \tag{13}$$

This boundary condition can also be described by equating the heat flux from both pipes, as:

$$q_i(L,t) = q_o(L,t) \tag{14}$$

where q_i and q_o are the heat flux going out of pipe-in and going in pipe-out, respectively.

3. General solution: the spectral analysis method

Many exact solution techniques have been developed for solving boundary value problems. Central among these is the transformation method. The Laplace transform is one of the best known and most widely used integral transformation technique. It is commonly used to produce an easily solvable ordinary differential equation from a partially differential equation by transforming it from a certain domain, usually time, to the Laplace domain. However, in most cases, finding the inverse transform, which is needed to reconstruct the time function back from the Laplace domain, is quite difficult, if possible, and usually numerical and asymptotic schemes are resorted in order to extract usable solutions.

An alternative transformation approach is the spectral analysis method (Doyle, 1997). In this approach, the continuous transform is approximated by the discrete Fourier transform. This transform possesses all the advantages of the forward transformation methods, adding to that, it is computational very efficient in the inverse transformation. The reconstruction of the time function from the transformed (frequency) domain can be accomplished very economically using the well-known FFT algorithm. This method has been widely utilized for solving wave propagation problems (Doyle, 1997).

The discrete transform of a space-time function entails the discretization of the dependent variable in the frequency and the spatial domains. The discretization in the frequency domain is commonly done by the FFT algorithm. The discretization in the spatial domain can be done by solving the homogeneous eigenfunction of the system to obtain its eigenvalues (wavenumbers). The general solution of the system can then be obtained by summing over all significant frequencies and wavenumbers.

Comparing this solution with solutions involving semi-infinite integration such as that typically involved in the inverse Laplace or Henkel transforms, two advantages can be deduced. First, the numerical evaluation of the involved integrals is replaced by simple algebraic summation. This is particularly important because the integrands involved are transcendental and their evaluation requires excessive computational demands. Second, the calculation of the system of equations in the spectral analysis method is performed only once for any number of output points. This means that the response of the system at any point can be calculated as a post-processing, without notable extra computational time. This is not the case in the integral formulations, where evaluation of the involved integrals must be done for each calculation point.

In this section, two spectral models are presented. The first model is formulated on the basis of the discrete Fourier transform, and the second model is formulated on the basis of the SEM. The two solution techniques are related, but the latter utilizes the finite element matrix formulation technique for solving the involved system of equations.

3.1 Model 1: discrete Fourier transform formulation

Equation (1) represents a system of coupled heat conduction-convection partial differential equations in space and time. This system of equations can be solved elegantly using the discrete Fourier transform method. A comprehensive treatment of this method for solving boundary value problems, mainly wave propagation, is covered in Doyle (1997). Here, the spectral procedure for solving coupled thermoelastic wave propagation proposed by Doyle (1988) is tailored to solve heat transfer in vertical BHEs.

A temperature function of time can be discretized as:

$$T(z,t_m)=\sum\nolimits_n \hat{T}(z,\omega_n)\,e^{i\omega_n t_m},\quad \hat{T}(z,\omega_n)=\frac{1}{N}\sum\nolimits_m T(z,t_m)\,e^{-i\omega_n t_m} \tag{15}$$

in which N is the number of the discrete samples, where in the FFT it is usually made $N = 2^{\gamma} = 2, 4, 8, \ldots, 2{,}048, \ldots$. For a real input signal, such as the one treated in this work, the transform is symmetric about a middle frequency, which is usually referred to as the Nyquist frequency. This means that N real points are transformed into $N/2$ complex points. For clarity of notation, the summation, the exponential term and the subscripts are ignored and the transform is represented here as $T \Leftrightarrow \hat{T}$.

Applying Equation (15) to Equation (1), the transformation from the time domain to the frequency domain leads to:

$$\begin{aligned} &i\omega\rho c\,\hat{T}_i\,dV_i - \lambda\frac{d^2\hat{T}_i}{dz^2}dV_i + \rho cu\frac{d\hat{T}_i}{dz}dV_i + b_{ig}(\hat{T}_i - \hat{T}_g)\,dS_{ig} = 0 \\ &i\omega\rho c\,\hat{T}_o\,dV_o - \lambda\frac{d^2\hat{T}_o}{dz^2}dV_o - \rho cu\frac{d\hat{T}_o}{dz}dV_o + b_{og}(\hat{T}_o - \hat{T}_g)\,dS_{og} = 0 \\ &i\omega\rho c_g\,\hat{T}_g\,dV_g - \lambda_g\frac{d^2\hat{T}_g}{dz^2}dV_g + b_{ig}(\hat{T}_g - \hat{T}_i)\,dS_{ig} + b_{og}(\hat{T}_g - \hat{T}_o)\,dS_{og} = 0 \end{aligned} \tag{16}$$

where it is obvious that the spectral representation of the time derivative:

$$\frac{\partial T}{\partial t} = \frac{\partial}{\partial t}\sum \hat{T}_n\,e^{i\omega_n t} = \sum i\,\omega_n\,\hat{T}_n\,e^{i\omega_n t} \tag{17}$$

has been replaced by:

$$\frac{\partial T}{\partial t} \Rightarrow i\omega\,\hat{T} \tag{18}$$

Similarly, the spatial derivatives are represented as:

$$\frac{\partial^m T}{\partial z^m} = \frac{\partial^m}{\partial z^m}\sum \hat{T}_n\,e^{i\omega_n t} = \sum \frac{\partial^m \hat{T}_n}{\partial z^m}\,e^{i\omega_n t} \Rightarrow \frac{\partial^m \hat{T}}{\partial z^m} \tag{19}$$

The utilization of the spectral approach has reduced the partial differential equations, Equation (1), to ordinary differential equations, by converting the time derivative to an algebraic expression. However, the resulting equations are frequency dependent and need to be solved for each frequency, ω_n.

The solution of the coupled system of equations, Equation (16), might have this form:

$$\hat{T}_i = A\,e^{-ikz}, \quad \hat{T}_g = \bar{A}\,e^{-ikz}, \quad \hat{T}_o = \overline{\overline{A}}\,e^{ikz}, \tag{20}$$

in which A, $\bar{A}$, $\overline{\overline{A}}$ are the integral constants and k denotes the wavenumber, which needs to be determined. It can be noticed from Equation (20) that the temperature in the pipe-in and the grout describes heat flow in the $z > 0$ direction, and the temperature in the pipe-out describes heat flow in the opposite direction (Figure 1).

Substituting Equation (20) into Equation (16) leads to:

$$\begin{aligned} &\lambda k^2 A\,dV_i - \rho cuikA\,dV_i + (i\omega\rho c\,dV_i + b_{ig}\,dS_{ig})A - b_{ig}\bar{A}\,dS_{ig} = 0 \\ &\lambda k^2\overline{\overline{A}}\,dV_o - \rho cuik\overline{\overline{A}}\,dV_o + (i\omega\rho c\,dV_o + b_{og}\,dS_{og})\overline{\overline{A}} - b_{og}\bar{A}\,e^{-2ikz}\,dS_{og} = 0 \\ &\lambda_g k^2\bar{A}\,dV_g + (i\omega\rho c_g\,dV_g + b_{ig}\,dS_{ig} + b_{og}\,dS_{og})\bar{A} - b_{ig}A\,dS_{ig} - b_{og}\overline{\overline{A}}\,e^{2ikz}\,dS_{og} = 0 \end{aligned} \tag{21}$$

In matrix form, Equation (21) can be written as:

$$\begin{pmatrix} \lambda k^2\, dV_i - \rho cuik\, dV_i + \\ i\omega\rho c\, dV_i + b_{ig}\, dS_{ig} & 0 & -b_{ig}\, dS_{ig} \\ -b_{ig}\, dS_{ig} & -b_{og}\, e^{2ikz}\, dS_{og} & \lambda_g k^2\, dV_g + i\omega\rho c_g\, dV_g + \\ & & b_{ig}\, dS_{ig} + b_{og}\, dS_{og} \\ 0 & \lambda k^2\, dV_o - \rho cuik\, dV_o + & -b_{og}\, e^{-2ikz}\, dS_{og} \\ & i\omega\rho c\, dV_o + b_{og}\, dS_{og} & \end{pmatrix} \times \begin{pmatrix} A \\ \overline{\overline{A}} \\ \bar{A} \end{pmatrix} = 0 \tag{22}$$

Non-trivial solution of Equation (22) can only be obtained by letting the determinate equal to zero, formulating a complex six-degree polynomial of the form:

$$a_6 k^6 + a_5 k^5 + a_4 k^4 + a_3 k^3 + a_2 k^2 + a_1 k + a_0 = 0 \tag{23}$$

from which the k values can be obtained by solving for its roots. This polynomial represents the eigenfunction of the BHE system with k denoting its set of eigenvalues (wavenumbers). Only for this set of eigenvalues do the eigenfunction exist that satisfies the boundary conditions of the problem. The exact forms of the constants of Equation (23) are listed in Appendix 1.

The determination of the wavenumbers must be done for every frequency. Six wavenumbers in three complex conjugates are obtained, representing three basic modes, one for each BHE component. Accordingly, the solution of the temperature distribution in the three BHE components can be written as:

$$\begin{aligned} \hat{T}_i &= A\, e^{-ik_1 z} + B\, e^{-ik_2 z} + C\, e^{-ik_3 z} \\ \hat{T}_g &= \bar{A}\, e^{-ik_1 z} + \bar{B}\, e^{-ik_2 z} + \bar{C}\, e^{-ik_3 z} \\ \hat{T}_o &= \overline{\overline{A}}\, e^{ik_1 z} + \overline{\overline{B}}\, e^{ik_2 z} + \overline{\overline{C}}\, e^{ik_3 z} \end{aligned} \tag{24}$$

where only flow of the heat sources is taken into consideration. Since T_i, T_g, and T_o are coupled, the integral constants, $A, B, \ldots, \overline{\overline{C}}$, are related to each other. The relationship between the pipe-in constants and the grout constants can be expressed, using Equation (22), as:

$$\bar{A} = \bar{Y} A \tag{25}$$

where

$$\bar{Y} = (\lambda k^2\, dV_i - \rho cuik\, dV_i + i\omega\rho c\, dV_i + b_{ig}\, dS_{ig}) / b_{ig}\, dS_{ig} \tag{26}$$

In the same way, the relationship between the pipe-out constants and the grout constants is:

$$\bar{A} = \overline{\overline{Y}}\,\overline{\overline{A}} \tag{27}$$

where,

$$\overline{\overline{Y}} = (\lambda k^2\, dV_o - \rho c u i k\, dV_o + i\omega\rho c\, dV_o + b_{og}\, dS_{og})/b_{og}\, e^{-2ikz}\, dS_{og} \tag{28}$$

For each k there is a corresponding $\bar{Y}$ and $\overline{\overline{Y}}$.

The integral constants, $A, B, \ldots, \overline{\overline{C}}$, of Equation (24) must be determined from the boundary conditions. The spectral representation of the boundary conditions, Equations (9), (10), and (13), can be expressed as:

$$\begin{aligned} \hat{T}_i(0,\omega) &= \hat{T}_{in}(\omega) \\ \lambda_g \frac{\partial \hat{T}_g(z,\omega)}{\partial z} &= b_{gs}[\hat{T}_g(z,\omega) - \hat{T}_s(z,\omega)] \\ \hat{T}_i(L,\omega) &= \hat{T}_o(L,\omega) \end{aligned} \tag{29}$$

The imposition of the third condition indicates that heat flow in the pipe-in is virtually continuing in the pipe-out, although it is in the opposite direction. This entails that the system is in effect consisting of two components, pipe-in and grout, that can be described basically by two modes. The third mode, which is related to pipe-out, would eventually diminish, i.e. $C = 0$. The proof of this result is given in Appendix 2. For $C = 0$ to be valid implicates that the properties of both pipes, pipe-in and pipe-out, such as geometry, material, and heat resistance must be identical. In practice, this is the case. The U-tube pipe is in-effect one pipe, which is inserted in a borehole and filled with the grout. This makes the properties of the two pipes identical. If, however, the two pipe properties are made different, especially that the heat resistance of pipe-in is made different from that for the pipe-out, i.e. $b_{ig} \neq b_{og}$, the BHE system needs to be treated as two sub-systems, one representing pipe-in-grout and another pipe-out-grout. The two sub-systems are coupled at the point where pipe-in and pipe-out meet, $z = L$. Equation (29) can then be expanded to become:

Pipe-in-grout:

$$\begin{aligned} \hat{T}_i(0,\omega) &= \hat{T}_{in}(\omega) \\ -\lambda_g \frac{\partial \hat{T}_{gi}(z,\omega)}{\partial z} &= -b_{gs}[\hat{T}_{gi}(z,\omega) - \hat{T}_s(z,\omega)] \end{aligned} \tag{30}$$

Pipe-out-grout:

$$\begin{aligned} \hat{T}_o(L,\omega) &= \hat{T}_i(L,\omega) \\ -\lambda_g \frac{\partial \hat{T}_{go}(z,\,\omega)}{\partial z} &= -b_{gs}[\hat{T}_{go}(z,\omega) - \hat{T}_s(z,\omega)] \end{aligned} \tag{31}$$

with the temperature in the grout taken as an average between the two sub-systems, as:

$$\hat{T}_g = \frac{1}{2}(\hat{T}_{gi} + \hat{T}_{go}) \tag{32}$$

where $\hat{T}_{gi}$ and $\hat{T}_{go}$ represent the grout temperature in contact with pipe-in and pipe-out, respectively.

Accordingly, Equation (24) can be modified to account for the two sub-systems, as:

Pipe-in-grout:

$$\begin{aligned}\hat{T}_i &= A_i\, e^{-ik_1 z} + B_i e^{-ik_2 z} \\ \hat{T}_{gi} &= \bar{A}_i\, e^{-ik_1 z} + \bar{B}_i\, e^{-ik_2 z}\end{aligned} \tag{33}$$

Pipe-out-grout:

$$\begin{aligned}\hat{T}_o &= A_o\, e^{ik_1 z} + B_o\, e^{ik_2 z} \\ \hat{T}_{go} &= \bar{A}_o\, e^{-ik_1 z} + \bar{B}_o\, e^{-ik_2 z}\end{aligned} \tag{34}$$

Substituting Equations (33) and (34) into Equations (30) and (31), and by assuming that soil temperature is constant along the z-axis, but might vary in time, results to:

Pipe-in-grout:

$$\begin{aligned}&A_i + B_i = \hat{T}_{in}(\omega) \\ &\left(ik_1 + \frac{b_{gs}}{\lambda_g}\right)\bar{A}_i\, e^{-ik_1 z} + \left(ik_2 + \frac{b_{gs}}{\lambda_g}\right)\bar{B}_i\, e^{-ik_2 z} = \frac{b_{gs}}{\lambda_g}\hat{T}_s(\omega)\end{aligned} \tag{35}$$

Pipe-out-grout:

$$\begin{aligned}&A_o\, e^{ik_1 L} + B_o\, e^{ik_2 L} = \hat{T}_i(L, \omega) \\ &\left(ik_1 + \frac{b_{gs}}{\lambda_g}\right)\bar{A}_o\, e^{-ik_1 z} + \left(ik_2 + \frac{b_{gs}}{\lambda_g}\right)\bar{B}_o\, e^{-ik_2 z} = \frac{b_{gs}}{\lambda_g}\hat{T}_s(\omega)\end{aligned} \tag{36}$$

Solving for A_i and B_i leads to:

$$A_i = \frac{\left(\left(ik_2 + \frac{b_{gs}}{\lambda_g}\right)\bar{Y}_2\, e^{-ik_2 z}\hat{T}_{in}(\omega) - \frac{b_{gs}}{\lambda_g}\hat{T}_s(\omega)\right)}{\left(ik_2 + \frac{b_{gs}}{\lambda_g}\right)\bar{Y}_2\, e^{-ik_2 z} - \left(ik_1 + \frac{b_{gs}}{\lambda_g}\right)\bar{Y}_1\, e^{-ik_1 z}} \tag{37}$$

$$B_i = \frac{\left(-\left(ik_1 + \frac{b_{gs}}{\lambda_g}\right)\bar{Y}_2\, e^{-ik_1 z}\hat{T}_{in}(\omega) + \frac{b_{gs}}{\lambda_g}\hat{T}_s(\omega)\right)}{\left(ik_2 + \frac{b_{gs}}{\lambda_g}\right)\bar{Y}_2\, e^{-ik_2 z} - \left(ik_1 + \frac{b_{gs}}{\lambda_g}\right)\bar{Y}_1\, e^{-ik_1 z}} \tag{38}$$

And solving for A_o and B_o, leads to:

$$A_o = \frac{\left(\left(ik_2 + \frac{b_{gs}}{\lambda_g}\right)\overline{\bar{Y}}_2\, e^{-ik_2 z}\,\hat{T}_i(L, \omega) - \frac{b_{gs}}{\lambda_g}\hat{T}_s(\omega)\right)}{\left(ik_2 + \frac{b_{gs}}{\lambda_g}\right)\overline{\bar{Y}}_2\, e^{-ik_2 z} - \left(ik_1 + \frac{b_{gs}}{\lambda_g}\right)\overline{\bar{Y}}_1\, e^{-ik_1 z}} e^{-ik_1 L} \tag{39}$$

$$B_o = \frac{\left(-\left(ik_1 + \frac{b_{gs}}{\lambda_g}\right)\overline{\overline{Y}}_2\, e^{-ik_1 z}\,\hat{T}_i(L,\omega) + \frac{b_{gs}}{\lambda_g}\hat{T}_s(\omega)\right)}{\left(ik_2 + \frac{b_{gs}}{\lambda_g}\right)\bar{Y}_2\, e^{-ik_2 z} - \left(ik_1 + \frac{b_{gs}}{\lambda_g}\right)\overline{\overline{Y}}_1\, e^{-ik_1 z}} e^{-ik_2 L} \tag{40}$$

where $\bar{Y}$ and $\overline{\overline{Y}}$ are as defined in Equations (26) and (28), with $\bar{Y}_1$ and $\overline{\overline{Y}}_1$ are associated with the wavenumber, k_1, and $\bar{Y}_2$ and $\overline{\overline{Y}}_2$ are associated with the wavenumber, k_2.

Having determined the eigenvalues and the integral constants, the general solution of the BHE system of equations can then be obtained by summing over of all significant modes (in this case two, k_1 and k_2) and frequencies as:

$$\begin{aligned} T_i(z,t) &= \sum\nolimits_n \left(A_i\, e^{-ik_1 z} + B_i\, e^{-ik_2 z}\right) e^{i\omega_n t} \\ T_o(z,t) &= \sum\nolimits_n \left(A_o\, e^{ik_1 z} + B_o\, e^{ik_2 z}\right) e^{i\omega_n t} \\ T_g(z,t) &= \frac{1}{2}\left[\sum\nolimits_n \left(\left(\bar{Y}_1 A_i + \overline{\overline{Y}}_1 A_o\right) e^{-ik_1 z} + \left(\bar{Y}_2 B_i + \overline{\overline{Y}}_2 B_o\right) e^{-ik_2 z}\right) e^{i\omega_n t}\right] \end{aligned} \tag{41}$$

The reconstruction of the time history can be done efficiently by the inverse FFT.

Variable soil temperature. In practice, soil temperature surrounding a BHE varies with depth. For any arbitrary distribution of soil temperature in space, it can be described using the complex Fourier series of the form:

$$T_s(z) = \sum\nolimits_m \hat{F}_m\, e^{-i\xi_m z} \tag{42}$$

in which,

$$\hat{F}_m = \frac{2\pi r_g}{L}\int_0^L T_s(z)\, e^{i\xi_m z}\, dz \tag{43}$$

where ξ_m represents the spatial modes of the soil temperature distribution along the axial axis. Incorporation of these modes in the system of equations (Equations (37)-(41)) implies the use of what is known as the Crosswise Superposition (reported by Tiomeshenko and Goodier, 1970), where Fourier series of different functions at different axial directions can be added. Accordingly, the general solution of the system of equations can be obtained by summing over all significant frequencies, eigenvalues, and soil spatial modes as:

$$\begin{aligned} T_i(z,t) &= \sum\nolimits_n \sum\nolimits_m \left(A_i\, e^{-ik_1 z} + B_i\, e^{-ik_2 z}\right)\hat{F}_m\, e^{i\omega_n t} \\ T_o(z,t) &= \sum\nolimits_n \sum\nolimits_m \left(A_o\, e^{ik_1 z} + B_o\, e^{ik_2 z}\right)\hat{F}_m\, e^{i\omega_n t} \\ T_g(z,t) &= \frac{1}{2}\left[\sum\nolimits_n \sum\nolimits_m \left(\left(\bar{Y}_1 A_i + \overline{\overline{Y}}_1 A_o\right)\hat{F}_m\, e^{-ik_1 z} + \left(\bar{Y}_2 B_i + \overline{\overline{Y}}_2 B_o\right)\hat{F}_m\, e^{-ik_2 z}\right) e^{i\omega_n t}\right] \end{aligned} \tag{44}$$

Summing over m can be made simply by an algebraic sum and over n can be made by the use of the inverse FFT.

Model verification. Verification of the model accuracy is illustrated by comparing its computational results with those obtained from an analytical solution of a simplified case.

So far, exact solution describing heat transfer in each individual BHE component and its thermal interactions with other components does not exist. However, the solution of a one-dimensional convective-dispersive solute transport, developed by van Genuchten and Alves (1982), can be utilized for solving heat transfer in a single one-dimensional (1D) pipe in contact with a surrounding medium, where a lateral heat exchange takes place. The temperature distribution of a fluid moving in a throw-off heat pipe and subjected to the following initial and boundary conditions:

$$T(z,t) = T_s; \quad T(0,t) = T_{in}; \quad \partial T(\infty,t)/\partial z = 0$$

is given by (see Diersch *et al.*, 2008):

$$T(z,t) = T_{in} - \frac{T_s - T_{in}}{2}\left\{e^{\frac{(u-v)z}{2D}}\operatorname{erfc}\left(\frac{z-vt}{2\sqrt{Dt}}\right) + e^{\frac{(u+v)z}{2D}}\operatorname{erfc}\left(\frac{z+vt}{2\sqrt{Dt}}\right)\right\} \tag{45}$$

in which erfc is the complementary error function, $D = \lambda/\rho c$ is the thermal diffusivity, u is the fluid velocity, and,

$$v = u\sqrt{1 + \frac{4\varphi D}{u^2}}$$

with $\varphi = 2\,b_{ig}/(r_i\,\rho c)$. T_s represents the temperature in the surrounding medium, soil in this case, and T_{in} represents the temperature of the fluid at the inlet of the pipe. The geometry and material parameters are as the following:

Pipe length	1 m
Pipe radius, r_i	0.013 m
Fluid ρc	4.1298E6 J/m^3 K
Fluid λ	0.38 W/m K
Fluid velocity, u	3.75E − 4 m/s
Pipe $b_{ig} = b_{gs}$	12 W/m^2 K

The external forces are: $T_s = 10\,^{\circ}\mathrm{C}$ and $T_{in} = 50\,^{\circ}\mathrm{C}$. This example is taken from Diersch *et al.* (2008), with the emphasis is to describe the model accuracy and capability to simulate heat transfer in short times.

In the spectral analysis, the external forces are described as:

$$T_{in}(t) = \begin{cases} 50 & 0 < t \le 3{,}000\,s \\ 0 & 3{,}000 < t < \infty\,s \end{cases}, \quad \text{and} \quad T_s(t) = 10 \quad 0 < t < \infty\,s \tag{46}$$

T_{in} is in effect equal to $T_s + \Delta T_{in}$, where is in this case $\Delta T_{in} = 40\,^{\circ}\mathrm{C}$. The temperature time histories of T_{in} and T_s were transformed to the frequency domain using the FFT algorithm. The number of transformation samples was 2,048, with a sample rate of 10 s, giving a time window of 20,480 s.

The calculation results of the temperature along the pipe after 1,728 s, as calculated by the van Genuchten model, Equation (45), and the spectral transform model, Equation (41), are shown in Figure 3. Apparently, the two results are nearly identical.

Figure 4 shows time reconstruction of the fluid temperature histories at different depths. As expected, the temperature is attenuated and the signal is propagating at a constant speed.

Another example is introduced here to examine the capability of the spectral model to describe the temperature distribution along the pipe-in and the pipe-out of a single U-tube BHE. Same geometry, material parameters and initial and boundary conditions as in the previous example were utilized. Two cases were studied. In one case the pipe-out-grout thermal coefficient, b_{og}, was made equal to b_{ig}, i.e. $b_{og} = 12\,\mathrm{W/m^2K}$, and in another case b_{og} was made very small, $b_{og} = 12\mathrm{E}-5\,\mathrm{W/m^2K}$. Figure 5 shows the temperature distribution in pipe-in and pipe-out for both cases. As expected, in the first

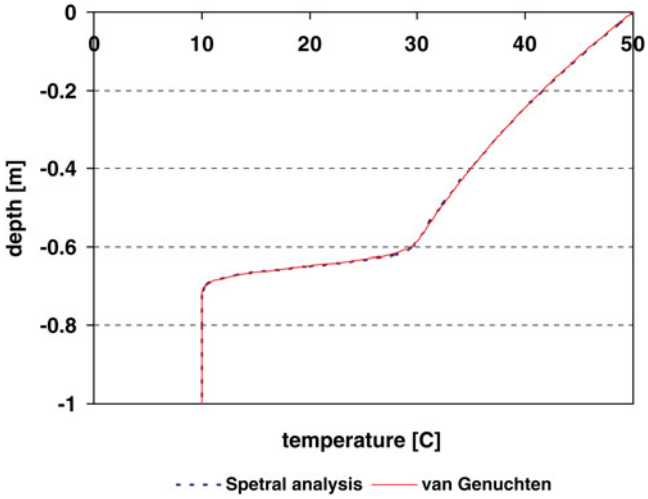

Figure 3.
Spectral analysis vs van Genuchten

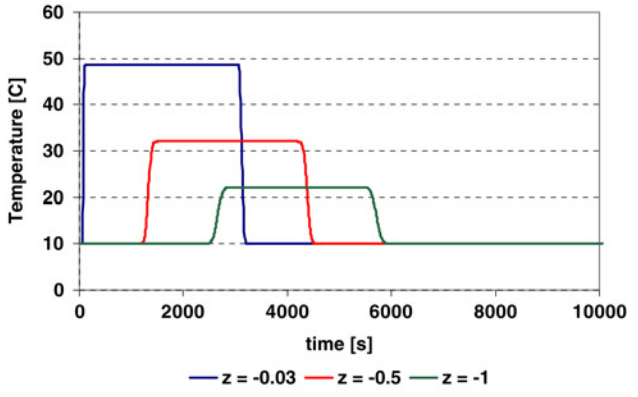

Figure 4.
Time snapshots for temperatures at different locations

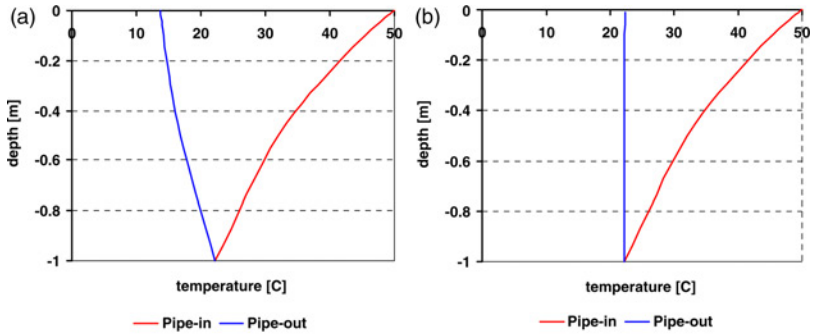

Figure 5.
Temperature distributions along pipe-in and pipe-out

Notes: (a) b_{og} = 12 W/m^2 K and (b) b_{og} = 12E–5 W/m^2 K

case, the fluid along pipe-out continues to interact with the surrounding medium, and hence the fluid temperature is continuously changing. In the second case, the fluid temperature at the bottom of pipe-in is kept the same throughout pipe-out. This indicates that pipe-out is totally insulated.

The grout temperature in both cases is equal to the soil temperature. This is a direct consequence of the second equation of Equation (29), where a one-way heat flux from the soil is prescribed. Variation in the grout temperature can only be realized if there is a two-way thermal interaction between the grout and the soil. This can be achieved if the BHE model is incorporated with a soil heat transfer model to describe a complete geothermal system. This will be the focus of a follow-up work.

3.2 Model 2: spectral element formulation

As an alternative way of utilizing the complex Fourier transform for describing the interaction between a BHE and a soil mass with variable temperature distribution, the SEM, developed by Doyle (1997), can be utilized. The SEM is a computationally efficient semi-numerical technique that makes use of the discrete Fourier transformation method and the finite element method. The basic difference from the finite element method is that the element stiffness (capacitance) matrix is described exactly. This entails that one element is sufficient to describe a whole layer or a member. Combination of many layers or members is made using the finite element matrix formulation and assembly techniques. Thus, this approach provides all the advantages of the spectral analysis method plus the efficiency of matrix organization of the finite element method.

The SEM is essentially developed for solving wave propagation problems (Doyle, 1997). Here, the SEM will be tailored to model heat transfer in a typical BHE in contact with a soil mass.

Unlike wave propagation problems, where reflection occurs at the boundary between different media, in heat transfer problems, no reflection takes place. This makes the spectral element of a BHE to consist of only one node, similar to that of the semi-infinite spectral element usually used in wave propagation problems (also called the throw-off element). The system of equations is solved at the node, but determination of the temperature at any point within the element can be done in the post-processing.

Following the discrete Fourier transform model, introduced in section 3.1, the temperatures in pipe-in, pipe-out, and grout can be described in the local coordinate system, ζ, as:

Pipe-in-grout:

$$\begin{aligned}\hat{T}_i &= A_i\, e^{-ik_1\zeta} + B_i\, e^{-ik_2\zeta} \\ \hat{T}_{gi} &= \bar{Y}_1 A_i\, e^{-ik_1\zeta} + \bar{Y}_2 B_i\, e^{-ik_2\zeta}\end{aligned} \tag{47}$$

Pipe-out-grout:

$$\begin{aligned}\hat{T}_o &= A_o\, e^{ik_1\zeta} + B_o\, e^{ik_2\zeta} \\ \hat{T}_{go} &= \overline{\overline{Y}}_1 A_o\, e^{-ik_1\zeta} + \overline{\overline{Y}}_2 B_o\, e^{-ik_2\zeta}\end{aligned} \tag{48}$$

in which the wavenumbers k_1 and k_2 can be determined from Equation (23). The spectral element is assumed to span from $\zeta = 0$ to $\zeta = h$, with h representing its length. In what follows, the pipe-in-grout system of equations, Equation (47), will be treated. The pipe-out-grout formulation follows suit.

At the element node, $\zeta = 0$, Equation (47) becomes:

$$\begin{pmatrix} \hat{T}_i \\ \hat{T}_{gi} \end{pmatrix} = \begin{pmatrix} 1 & 1 \\ \bar{Y}_1 & \bar{Y}_2 \end{pmatrix} \begin{pmatrix} A_i \\ B_i \end{pmatrix} \tag{49}$$

In compact form, Equation (49) can be written as:

$$\mathbf{A} = \mathbf{Q}^{-1}\hat{\mathbf{T}} \tag{50}$$

The corresponding heat fluxes in the pipe-in and the grout are:

$$\hat{q}_i = -\lambda \frac{\partial \hat{T}_i}{\partial z}\, dV_i + \rho cu\, \hat{T}_i\, dV_i \tag{51}$$

$$\hat{q}_{gi} = -\lambda_g \frac{\partial \hat{T}_{gi}}{\partial z} \tag{52}$$

Considering the thermal interaction between the grout and the soil, the Newton's law of cooling can be utilized such that:

$$\hat{q}_{gi} = -\lambda_g \frac{\partial \hat{T}_{gi}}{\partial z} = -b_{gs}[\hat{T}_{gi} - \hat{T}_s(z,\omega)] \tag{53}$$

Substituting Equation (47) into Equations (51) and (53) results to:

$$\begin{aligned}\hat{q}_i &= (i\,k_1\lambda e^{-i\,k_1\zeta} + \rho cue^{-i\,k_1\zeta})\, dV_i A_i + (ik_2\lambda\, e^{-i\,k_2\zeta} + \rho cue^{-i\,k_2\zeta})\, dV_i B_i \\ \hat{q}_{gs} &= (i\,k_1\lambda_g\, \bar{Y}_1\, e^{-i\,k_1\zeta} + \bar{Y}_1\, e^{-i\,k_1\zeta}\, b_{gs}) A_i + (i\,k_2\,\lambda_g\, \bar{Y}_2\, e^{-i\,k_2\zeta} + \bar{Y}_2\, e^{-i\,k_2\zeta} b_{gs})\, B_i\end{aligned} \tag{54}$$

in which $\hat{q}_{gs} = b_{gs}\, \hat{T}_s(z,\omega)$.

In the first element, where the element node is at $\zeta = z = 0$, $\hat{q}_i = \hat{q}_{in}$, the element heat flux equations, Equation (54), can be written as:

$$\begin{pmatrix} \hat{q}_{in} \\ \hat{q}_{gs} \end{pmatrix} = \begin{pmatrix} i\,k_1 \lambda \mathrm{A} + \rho cu\,\mathrm{A} & i\,k_2 \lambda \mathrm{A} + \rho cu\,\mathrm{A} \\ i\,k_1 \lambda_g\,\bar{Y}_1 + \bar{Y}_1\,b_{gs} & i\,k_2 \lambda_g\,\bar{Y}_2 + \bar{Y}_2\,b_{gs} \end{pmatrix} \begin{pmatrix} A_i \\ B_i \end{pmatrix} \tag{55}$$

in which A is the cross-sectional area of the pipe-in. Equation (55) can be written in vector notation as:

$$\hat{\mathbf{q}} = \hat{\mathbf{M}}\,\mathbf{A} \tag{56}$$

Substituting vector $\mathbf{A}$ from Equation (50) into Equation (56) leads to:

$$\hat{\mathbf{q}} = \hat{\mathbf{M}}\,\mathbf{Q}^{-1}\,\hat{\mathbf{T}} = \hat{\mathbf{K}}\,\hat{\mathbf{T}} \tag{57}$$

in which $\hat{\mathbf{K}}$ is equivalent to the stiffness or capacitance matrix in the finite element method, but here described exactly in the frequency domain.

Solving Equation (57), the temperatures of pipe-in and grout at the node can be determined. Once the temperature at the node is obtained, the integral coefficients A_i and B_i can be determined from Equation (50), and the temperature at any point along the length of the element can be calculated using Equation (47).

For a system consisting of more than one element, a sequential determination of the temperatures is required. This differs from classical spectral element technique where element assembly is required. Here, the continuity condition between two sequential elements, j and $j+1$, is imposed at $\zeta = h$, such that:

$$\hat{q}_i^{\,j+1}(0,\omega) = \hat{q}_i^{\,j}(h,\omega) \tag{58}$$

The heat flux equations, Equation (55), for element $j+1$ can then be described as:

$$\begin{pmatrix} \hat{q}_i^{\,j}(h,\omega) \\ \hat{q}_{gs}^{\,j+1} \end{pmatrix} = \begin{pmatrix} i\,k_1^{j+1} \lambda\,\mathrm{A} + \rho cu\,\mathrm{A} & i\,k_2^{j+1} \lambda \mathrm{A} + \rho cu\,\mathrm{A} \\ i\,k_1^{j+1} \lambda_g\,\bar{Y}_1 + \bar{Y}_1\,b_{gs} & i\,k_2^{j+1} \lambda_g\,\bar{Y}_2 + \bar{Y}_2\,b_{gs} \end{pmatrix} \begin{pmatrix} A_i^{j+1} \\ B_i^{j+1} \end{pmatrix} \tag{59}$$

in which the wavenumbers of element $j+1$ need to be determined from Equation (23). The corresponding temperature distribution in pipe-in and the grout is described as:

$$\begin{pmatrix} \hat{T}_i^{j+1} \\ \hat{T}_g^{j+1} \end{pmatrix} = \begin{pmatrix} e^{-i\,k_1^{j+1}\zeta} & e^{-i\,k_2^{j+1}\zeta} \\ \bar{Y}_1\,e^{-i\,k_1^{j+1}\zeta} & \bar{Y}_2\,e^{-i\,k_2^{j+1}\zeta} \end{pmatrix} \begin{pmatrix} A_i^{j+1} \\ B_i^{j+1} \end{pmatrix} \tag{60}$$

By substituting the coefficients A_i^{j+1} and B_i^{j+1} from Equation (59) into Equation (60) the temperatures at any point along element $j+1$ can be determined. The same procedure can be followed for all elements involved.

The general solution of a system subjected to an external heat flux or prescribed temperature of the type $\hat{T}(\xi,\omega) = \hat{F}_m(\xi)\hat{F}_n(\omega)$, with $\hat{F}_m(\xi)$ representing the spatial distribution of the force and $\hat{F}(\omega)$ representing its frequency spectrum, can be solved by summing over all significant spatial modes and frequencies. The general solution of a BHE system of equations can be described as:

$$\mathbf{T}(z,t) = \sum\nolimits_n \sum\nolimits_m \hat{\mathbf{G}}(k_m,\omega_n)\hat{F}_m\,\hat{F}_n\,e^{i\,\omega_n t} \tag{61}$$

in which $\hat{\mathbf{G}}(k_m, \omega_n) = \hat{\mathbf{K}}(k_m, \omega_n)^{-1}$ representing the transfer function of the system. In case of a prescribed temperature at the inlet of pipe-in, $\hat{T}_{in}, \hat{F}_m = 1$, and $\hat{F}_n$ is calculated by means of the FFT algorithm. For a time varying soil temperature and a constant distribution in space, the same is valid. However, for a varying soil temperature in space a crosswise superposition, as described in the previous section, must be used for each element.

Element verification. The van Genuchten solution of a single 1D heat pipe, described in section 3.1, is utilized here to verify the spectral element model. The pipe is simulated using one spectral element. Material and geometrical properties identical to those utilized in the previous example are used here. The calculation results obtained from the spectral element model together with the van Genuchten solution are shown in Figure 6. Apparently there is a quite good match between the two results.

Figure 6 also shows two finite element calculation results conducted by Diersch *et al.* (2008), using the FEFLOW finite element package. Part of the finite element mesh is shown in Figure 7, where a cut along the BHE is made. Two mesh coarseness along the vertical axis were utilized: one using 100 elements (slices) and another using 200 elements. The dimension of the mesh is 20 m × 20 m × 1 m. The heat transfer coefficients of pipe-in and the grout are made equal, $b_{ig} = b_{gs}$, while heat transfer in pipe-out is set to zero, $b_{og} = 0$, to eliminate its thermal interaction with other pipe components. The temperature in the soil is kept constant. All other parameters are as described in the previous example.

The figure shows that even though the finite element results are in good agreement with the analytical solution, the spectral element results are more accurate. Adding to that, the spectral element model is remarkably efficient. The SEM required only one element to describe the whole pipe, while the finite element method needed 200 elements (in the vertical direction) to come close, but not too close, to the analytical solution.

It might be useful to indicate here that FEFLOW incorporates the BHE model introduced in Al-Khoury *et al.* (2005) and Al-Khoury and Bonnier (2006). This model is capable of reducing the amount of finite elements in the radial direction significantly. However, in the vertical direction, relatively fine mesh might be needed for short time analysis, such as the one presented here.

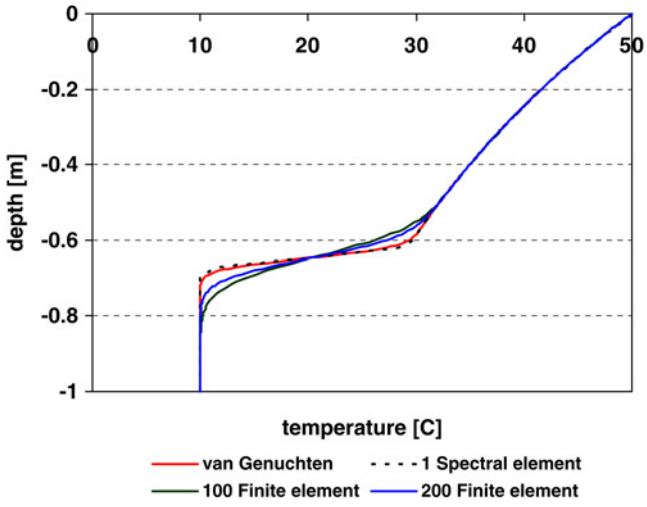

Figure 6.
SEM vs van Genuchten solution and finite element solutions

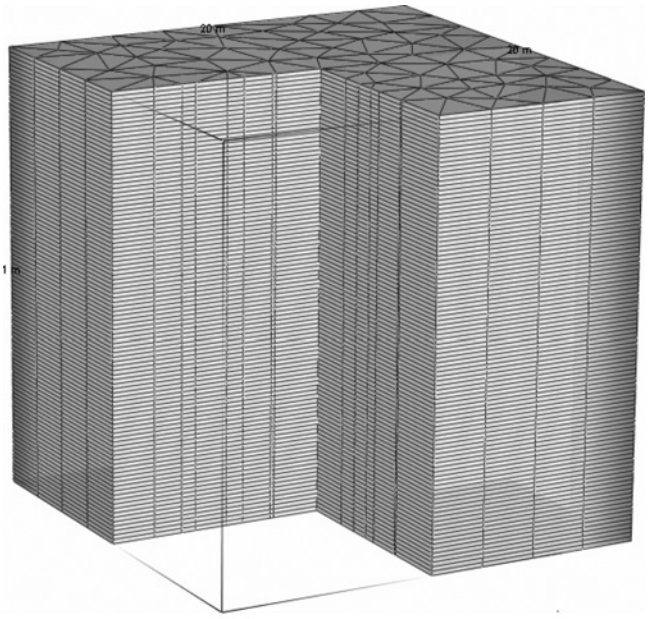

Source: Diersch *et al.* (2008)

Figure 7.
A cut along the BHE in the finite element mesh

4. Conclusions

Vertical BHEs are extremely slender geothermal heat pipes. The slenderness makes their installation in the ground relatively easy. However, it exerts considerable computational challenges, especially when numerical methods are utilized. In spite of some successful attempts for circumventing this problem, analytical and semi-numerical methods are nevertheless preferable in engineering practice. For this, in this publication, a framework is established for deriving analytical and semi-numerical models for conductive-convective heat transfer in a typical U-tube BHE and its thermal interaction with a soil mass. The spectral analysis method is utilized. This method possesses all the advantages of the forward transform methods. Added to that, the spectral analysis method is extremely efficient in the inverse transform, which can be done economically and robustly using the FFT algorithm.

Two spectral analysis models are introduced. The first model describes heat transfer in a single U-tube borehole exchanger in contact with a soil mass using the discrete Fourier transform method. The formulation is general such that the external forces, mainly the temperature or the heat flux of the refrigerant at the inlet of pipe-in, can vary with time. The soil mass temperature can vary in time and space.

The second model is derived on the basis of the SEM. This method allows for the simulation of a BHE in contact with a multilayer system. The number of spectral elements can be as many as the number of layers involved. This method retains all the advantages of the discrete Fourier transform, in addition to the efficiency of the matrix formulation and assembly of the finite element method.

Verification and numerical examples have shown that the developed models are extremely accurate and computationally very efficient. It was shown that one spectral element could produce results which are more accurate than those produced by 200 finite elements.

The introduced models are generic and can be used as a framework for developing more comprehensive models for shallow geothermal systems consisting of multiple BHEs embedded in multilayer soil systems. Different techniques, such as analytical, semi-analytical, or numerical, can be used to model heat transfer in the soil mass. The thermal interaction between the soil mass and the boreholes can be done by the use of a staggered (sequential) algorithm, wherein the system is divided into two sub-systems: one representing the BHEs and the other representing the soil. The two systems are solved separately, but connected in their external forces, i.e. heat fluxes at their boundary surfaces.

The BHE models can also be extended to model coaxial and double U-tube BHE's. In a follow up paper, some of these issues will be addressed.

References

Al-Khoury, R. and Bonnier, P.G. (2006), "Efficient finite element formulation for geothermal heating systems. Part II: transient", *International Journal for Numerical Methods in Engineering*, Vol. 67, pp. 725-45.

Al-Khoury, R., Bonnier, P.G. and Brinkgreve, R.B.J. (2005), "Efficient finite element formulation for geothermal heating systems. Part I: steady state", *International Journal for Numerical Methods in Engineering*, Vol. 63, pp. 988-1013.

Carslaw, H.S. and Jaeger, J.C. (1947), *Conduction of Heat in Solids*, Oxford University Press, London.

Clauser, C. (Ed.) (2003), *Numerical Simulation of Reactive Flow in Hot Aquifers: SHEMAT and Processing SHEMAT*, Springer, Heidelberg.

Diersch, H.-J.G., Ruhaak, W., Schatzl, P. and Renz, A. (2008), "A new method for modelling geothermal heat exchangers in shallow aquifer systems", working paper, DHI-WASY GmbH, Berlin, available at: www.feflow.info

Doyle, J.F. (1988), "Spectral analysis of coupled thermoelastic waves", *Journal of Thermal Stresses*, Vol. 11, pp. 175-85.

Doyle, J.F. (1997), *Wave Propagation in Structures: Spectral Analysis Using Fast Discrete Fourier Transforms*, Springer-Verlag, New York, NY.

Eskilson, P. and Claesson, J. (1988), "Simulation model for thermally interacting heat extraction boreholes", *Numerical Heat Transfer*, Vol. 13, pp. 149-65.

Ingersoll, L.R., Zobel, O.J. and Ingersoll, A.C. (1954), *Heat Conduction with Engineering, Geological, and other Applications*, revised ed., University of Wisconsin Press, Madison, WI.

Marcotte, D. and Pasquier, P. (2008), "Fast fluid and ground temperature computation for geothermal ground-loop heat exchanger systems", *Geothermics*, Vol. 37, pp. 651-65.

Marcotte, D. and Pasquier, P. (2009), "The effect of borehole inclination on fluid and ground temperature", *Geothermics*, Vol. 38 No. 4, pp. 392-8.

Muraya, N.K. (1994), "Numerical modelling of the transient thermal interface of vertical U-tube heat exchangers", PhD thesis, Texas A&M University, College Station, TX.

Sliwa, T. and Gonet, A. (2005), "Theoretical model of borehole heat exchanger", *Journal of Energy Resources Technology, ASME*, Vol. 27, pp. 142-8.

Sutton, M., Nutter, D. and Couvillion, R. (2003), "A ground resistance for vertical bore heat exchangers with groundwater flow", *Journal of Energy Resources Technology*, Vol. 125, pp. 183-9.

Timoshenko, S.P. and Goodier, J.N. (1970), *Theory of Elasticity*, 3rd ed., McGraw-Hill, New York, NY.

van Genuchten, M.Th. and Alves, W.J. (1982), "Analytical solutions of the one-dimensional convective-dispersive solute transport equation", Technical Bulletin No. 1661, US Department of Agriculture, Washington, DC.

Yavuzturk, C. and Spitler, J. (1999), "A short time step response factor model for vertical ground loop heat exchangers", *ASHRAE Transaction*, Vol. 105, pp. 475-85.

Zeng, H., Diao, N. and Fang, Z. (2002), "A finite line-source model for boreholes in geothermal heat exchangers", *Heat Transfer-Asian Research*, Vol. 31, pp. 558-67.

Zeng, H., Diao, N. and Fang, Z. (2003), "Heat transfer analysis of boreholes in vertical ground heat exchangers", *International Journal of Heat and Mass Transfer*, Vol. 46, pp. 4467-81.

Appendix 1

The eigenfunction of the BHE system is described in Equation (23), as:

$$a_6 k^6 + a_5 k^5 + a_4 k^4 + a_3 k^3 + a_2 k^2 + a_1 k + a_0 = 0 \tag{A1.1}$$

The exact forms of the involved constants are:

$$\begin{aligned}
a_6 &= \lambda^2 \lambda_g \, dV_i \, dV_o \, dV_g \\
a_5 &= -2i\lambda\lambda_g \rho c u \, dV_i \, dV_o \, dV_g \\
a_4 &= b_{ig}\lambda_g \lambda \, dS_{ig} \, dV_g \, dV_o - \rho^2 c^2 u^2 \lambda_g \, dV_i \, dV_g \, dV_o + 2i\lambda\lambda_g \omega \rho c \, dV_i \, dV_g \, dV_o \\
&\quad + \lambda^2 b_{og} \, dV_i \, dS_{og} \, dV_o + \lambda\lambda_g b_{og} \, dV_i \, dS_{og} \, dV_g + i\lambda^2 \omega \rho_g c_g \, dV_i \, dV_g \, dV_o \\
&\quad + \lambda^2 b_{ig} \, dV_i \, dS_{ig} \, dV_o \\
a_3 &= 2\rho^2 c^2 u \lambda_g \omega \, dV_i \, dV_g \, dV_o - i\rho c u \lambda_g b_{og} \, dV_i \, dV_g \, dS_{og} - i b_{ig} \lambda_g \rho c u \, dV_o \, dV_g \, dS_{ig} \\
&\quad - 2i\lambda \, b_{og} \rho c u \, dV_o \, dV_i \, dS_{og} + 2\lambda \rho c u \omega \rho_g c_g \, dV_o \, dV_i \, dV_g - 2i\lambda \, b_{ig} \rho c u \, dV_o \, dV_i \, dS_{ig} \\
a_2 &= \lambda b_{ig} b_{og} \, dV_i \, dS_{ig} \, dS_{og} - 2i\lambda b_{ig} \omega \rho c \, dV_i \, dV_o \, dS_{ig} - \omega^2 \rho^2 c^2 \lambda_g \, dV_i \, dV_o \, dV_g \\
&\quad + i \, b_{ig} \omega \rho_g c_g \lambda \, dV_g \, dV_o \, dS_{ig} - 2\lambda\omega^2 \rho_g c_g \rho c \, dV_i \, dV_o \, dV_g - \rho^2 c^2 u^2 b_{ig} \, dV_i \, dV_o \, dS_{ig} \\
&\quad + i\omega \rho c \lambda_g b_{og} \, dV_i \, dV_g \, dS_{og} + b_{ig} b_{og} \lambda_g \, dS_{ig} \, dV_g \, dS_{og} - \rho^2 c^2 u^2 b_{og} \, dV_i \, dV_o \, dS_{og} \\
&\quad + b_{ig} b_{og} \lambda \, dS_{ig} \, dV_o \, dS_{og} + 2i\lambda b_{og} \omega \rho c \, dV_i \, dV_o \, dS_{og} + i b_{ig} \lambda_g \omega \rho c \, dV_g \, dV_o \, dS_{ig} \\
&\quad + i\lambda \omega \rho_g c_g b_{og} \, dV_i \, dV_g \, dS_{og} - i\rho^2 c^2 u^2 \omega \, \rho_g c_g \, dV_i \, dV_o \, dV_g \\
a_1 &= 2i\rho^2 c^2 u \omega^2 \rho_g c_g \, dV_i \, dV_o \, dV_g - i b_{ig} b_{og} \rho c u \, dV_o \, dS_{ig} \, dS_{og} + \rho c u \omega \rho_g c_g b_{og} \, dV_i \, dV_g \, dS_{og} \\
&\quad + 2\rho^2 c^2 u \omega b_{ig} \, dV_i \, dV_o \, dS_{ig} + 2\rho^2 c^2 u \omega b_{og} \, dV_i \, dV_o \, dS_{og} + b_{ig} \omega \rho_g c_g \rho c u \, dV_o \, dV_g \, dS_{ig} \\
&\quad - i\rho c u b_{ig} b_{og} \, dV_i \, dS_{ig} \, dS_{og} \\
a_0 &= -i\omega^3 \rho^2 c^2 \, \rho_g c_g \, dV_i \, dV_o \, dV_g - \omega^2 \rho^2 c^2 b_{og} \, dV_i \, dV_o \, dS_{og} - \omega^2 \rho^2 c^2 b_{ig} \, dV_i \, dV_o \, dS_{ig} \\
&\quad - \omega^2 \rho c \rho_g c_g b_{og} \, dV_i \, dV_g \, dS_{og} + i\omega \rho c b_{ig} b_{og} \, dV_i \, dS_{ig} \, dS_{og} + i\omega \rho c b_{ig} b_{og} \, dV_o \, dS_{ig} \, dS_{og} \\
&\quad + i b_{ig} \omega \rho_g c_g b_{og} \, dV_g \, dS_{ig} \, dS_{og} - b_{ig} \omega^2 \rho_g c_g \rho c \, dV_o \, dV_g \, dS_{ig}
\end{aligned}$$

The convenient form of Equation (A1.1) was obtained using Maple software (see MAPLE 12.0. Maplesoft, Waterloo Maple Inc, available at: www.maplesoft.com). Solution of Equation (A1.1) has been conducted using the IMSL mathematical library subroutine for finding the zeros of polynomials of complex coefficients, DZPOCC (see IMSL, Fortran Numerical Library. MATH/LIBRARY, 6.0, available at: www.intel.com).

Appendix 2

The relationship between the pipe-in and pipe-out integral coefficients can be determined from the third boundary condition, Equation (13). The spectral representation of Equation (13) is:

$$\hat{T}_i(L, \omega) = \hat{T}_o(L, \omega) \tag{A2.1}$$

Substituting Equation (20) into Equation (A2.1) results to:

$$A\,e^{-ikL} = \overline{\overline{A}}\,e^{ikL} \tag{A2.2}$$

Equation (A2.2) can be written as:

$$\overline{\overline{A}} = A\,e^{-2ikL}$$

This is valid for all integral constants such that:

$$\begin{aligned} \overline{\overline{A}} &= A\,e^{-2ik_1L} \\ \overline{\overline{B}} &= B\,e^{-2ik_2L} \\ \overline{\overline{C}} &= C\,e^{-2ik_3L} \end{aligned} \tag{A2.3}$$

Substituting Equation (A2.3) into Equation (A2.1), and using Equation (24), leads to:

$$A\,e^{-ik_1L} + B\,e^{-ik_2L} + C\,e^{-ik_3L} = A\,e^{-2ik_1L}\,e^{ik_1L} + B\,e^{-2ik_2L}\,e^{ik_2L} + C\,e^{-2ik_3L}\,e^{ik_3L} \tag{A2.4}$$

The spectral representation of the boundary conditions, Equations (9) and (10), can be written as:

$$\begin{aligned} &\hat{T}_i(0,\omega) = \hat{T}_{in}(\omega) \\ &-\lambda_g \frac{\partial \hat{T}_g(z,\omega)}{\partial z} = -b_{gs}(\hat{T}_g - \hat{T}_s) \end{aligned} \tag{A2.5}$$

The soil temperature is assumed constant along the z-axis, but might vary in time. Substituting Equations (24) into Equations (A2.5) results to:

$$\begin{aligned} &A + B + C = \hat{T}_{in} \\ &\left(ik_1 + \frac{b_{gs}}{\lambda_g}\right)\bar{A}\,e^{-ik_1z} + \left(ik_2 + \frac{b_{gs}}{\lambda_g}\right)\bar{B}\,e^{-ik_2z} + \left(ik_3 + \frac{b_{gs}}{\lambda_g}\right)\bar{C}\,e^{-ik_3z} = \frac{b_{gs}}{\lambda_g}\hat{T}_s \end{aligned} \tag{A2.6}$$

Putting Equations (A2.6) and (A2.4) in a matrix format results to:

$$\begin{pmatrix} 1 & 1 & 1 \\ \left(ik_1 + \frac{b_{gs}}{\lambda_g}\right)\bar{Y}_1\,e^{-ik_1z} & \left(ik_2 + \frac{b_{gs}}{\lambda_g}\right)\bar{Y}_2\,e^{-ik_2z} & \left(ik_3 + \frac{b_{gs}}{\lambda_g}\right)\bar{Y}_3\,e^{-ik_3z} \\ 0 & 0 & 0 \end{pmatrix} \begin{pmatrix} A \\ B \\ C \end{pmatrix} = \begin{pmatrix} \hat{T}_{in} \\ \frac{b_{gs}}{\lambda_g}\hat{T}_s \\ 0 \end{pmatrix} \tag{A2.7}$$

This equation leads to $C = 0$.

Corresponding author
Rafid Al-Khoury can be contacted at: r.i.n.alkhoury@tudelft.nl